

# T cell receptor ligation induces the formation of dynamically regulated signaling assemblies

Stephen C. Bunnell,<sup>1</sup> David I. Hong,<sup>1</sup> Julia R. Kardon,<sup>1</sup> Tetsuo Yamazaki,<sup>1</sup> C. Jane McGlade,<sup>2</sup> Valarie A. Barr,<sup>1</sup> and Lawrence E. Samelson<sup>1</sup>

<sup>1</sup>Laboratory of Cellular and Molecular Biology, Center for Cancer Research, National Cancer Institute, National Institutes of Health, Bethesda, MD 20892

<sup>2</sup>Department of Medical Biophysics and Program in Cell Biology, Hospital for Sick Children, Toronto, Ontario M5G 1X8, Canada

**T** cell antigen receptor (TCR) ligation initiates tyrosine kinase activation, signaling complex assembly, and immune synapse formation. Here, we studied the kinetics and mechanics of signaling complex formation in live Jurkat leukemic T cells using signaling proteins fluorescently tagged with variants of enhanced GFP (EGFP). Within seconds of contacting coverslips coated with stimulatory antibodies, T cells developed small, dynamically regulated clusters which were enriched in the TCR, phosphotyrosine, ZAP-70, LAT, Grb2, Gads, and SLP-76, excluded the lipid raft marker enhanced yellow fluorescent protein–GPI, and

were competent to induce calcium elevations. LAT, Grb2, and Gads were transiently associated with the TCR. Although ZAP-70-containing clusters persisted for more than 20 min, photobleaching studies revealed that ZAP-70 continuously dissociated from and returned to these complexes. Strikingly, SLP-76 translocated to a perinuclear structure after clustering with the TCR. Our results emphasize the dynamically changing composition of signaling complexes and indicate that these complexes can form within seconds of TCR engagement, in the absence of either lipid raft aggregation or the formation of a central TCR-rich cluster.

## Introduction

Signaling pathways activated after engagement of the T cell antigen receptor (TCR)\* have been studied using biochemical techniques for over a decade (for review see Koretzky and Myung, 2001; Yablonski and Weiss, 2001; Samelson, 2002). Signaling downstream of the TCR is initiated when the signal-transducing subunits (CD3 and TCR $\zeta$ ) of engaged TCRs are phosphorylated by the Src-family protein tyrosine kinases (PTKs) Lck and Fyn. These modifications occur within immunoreceptor tyrosine-based activation motifs and direct the recruitment of ZAP-70, a Syk-family PTK, to the TCR

via its tandem Src-homology 2 domains. Once recruited, ZAP-70 is phosphorylated and activated by Lck and Fyn. Activated ZAP-70 phosphorylates several substrates, including LAT and SLP-76, adapter proteins required for optimal T cell activation and development (Finco et al., 1998; Yablonski et al., 1998; Zhang et al., 1999). The phosphorylation of LAT, a lipid raft-associated integral membrane protein, creates docking sites for various Src-homology 2 domains. PLC- $\gamma$ 1 and the adapters Grb2, Grap, and Gads bind to LAT in this manner (Zhang et al., 1998a). SLP-76 is also recruited into LAT-nucleated complexes through its interaction with the COOH-terminal SH3 domain of Gads (Liu et al., 1999). SLP-76 provides an additional platform for the recruitment of signaling molecules, including PLC- $\gamma$ 1, the Rho-family GTPase nucleotide exchange factor Vav, the adapter Nck, and the Tec-family tyrosine kinase Itk (Wu et al., 1996; Bubeck Wardenburg et al., 1998; Bunnell et al., 2000; Yablonski et al., 2001). c-Cbl, an adapter and ubiquitin ligase, also associates with LAT, although by an undefined mechanism (Zhang et al., 1998a). Because these associations have primarily been defined in coimmunoprecipitation studies, relatively little is known about the initiation, maturation, dynamic composition, and stoichiometry of these complexes.

Various imaging studies have established that T cells that engage antigen-presenting cells (APCs) bearing stimulatory

The online version of this paper contains supplemental material.

Address correspondence to Lawrence Samelson, Laboratory of Cellular and Molecular Biology, Center for Cancer Research, National Cancer Institute, National Institutes of Health, Bldg. 37, Rm. 1E24, Bethesda, MD 20892. Tel.: (301) 496-9683. Fax: (301) 496-8479.

E-mail: samelson@helix.nih.gov

\*Abbreviations used in this paper: APC, antigen-presenting cell; cSMAC, central supramolecular activation cluster; EGFP, enhanced GFP; EYFP, enhanced yellow fluorescent protein; IRM, interference reflection microscopy; pSMAC, peripheral SMAC; PTK, protein tyrosine kinase; TCR, T cell receptor; Th2 cells, T helper 2 CD4-positive T cells.

Tetsuo Yamazaki's present address is Dept. of Molecular Genetics, Institute for Liver Research, Kansai Medical University, Moriguchi, Osaka 570-8506, Japan.

Key words: T cell receptor; adapters; signaling complexes; tyrosine phosphorylation; confocal microscopy

MHC-peptide complexes undergo macromolecular rearrangements that result in the formation of an immune synapse. This structure develops over 5–30 min as a result of active cytoskeletal processes and subdivides the T cell–APC interface into two concentric zones: the central and peripheral supramolecular activation clusters (cSMAC and pSMAC) (for review see Delon and Germain, 2000). The cSMAC is enriched in the TCR, CD2, and CD28, whereas the pSMAC contains integrins and cytoskeletal proteins. Larger glycoproteins, such as CD43 and CD45, are initially excluded from the entire synapse (Sperling et al., 1998; Johnson et al., 2000). Despite the dramatic nature of these rearrangements, the function of the immune synapse remains elusive.

Initial reports describing the immune synapse emphasized the correlation between SMAC formation and productive T cell activation (Monks et al., 1998; Grakoui et al., 1999). However, neither thymocytes nor T helper 2 CD4-positive T cells (Th2) cells develop immune synapses during their activation (Balamuth et al., 2001; Richie et al., 2002). Additionally, increases in cellular phosphotyrosine, intracellular calcium elevations, the dephosphorylation of moesin, and cytoskeletal rearrangements are all initiated within seconds of receptor engagement and peak within 2 to 3 min of TCR engagement (Negulescu et al., 1996; Wulfiging and Davis, 1998; Bunnell et al., 2001; Delon et al., 2001). Therefore, the signals driving these events must be derived from TCRs ligated before the formation of a cSMAC (Monks et al., 1998; Grakoui et al., 1999; Dustin and Cooper, 2000; Lee et al., 2002). Several reports have indicated that TCRs are initially engaged at the periphery of the T cell–APC contact or in small clusters within the maturing synapse (Grakoui et al., 1999; Dustin and Cooper, 2000; Krummel and Davis, 2002). More recently, peak levels of activated Lck and ZAP-70 were found with the TCR in a peripheral zone before the coalescence of the engaged TCRs into a cSMAC (Lee et al., 2002), suggesting that signal transduction is initiated in these small, TCR-rich clusters, before the formation of a mature SMAC.

Dynamic studies of high temporal resolution are needed to relate the biochemical events described above to the complex morphological changes associated with T cell activation. To this end, we adapted a method developed in order

to simultaneously visualize T cell contacts and the rearrangement of enhanced GFP (EGFP)-tagged actin in live, activated T cells (Bunnell et al., 2001). This approach constrains responding T cells to the plane of a stimulatory coverslip, allowing the rapid collection of high-resolution images of chimeric proteins participating in signaling complexes within developing contacts. Our results establish that fully functional signaling complexes form rapidly within membrane domains tightly associated with the stimulatory surface, that components of these complexes are continuously dissociating and reassociating, and that the components of these complexes exit by distinct mechanisms. These results reveal both the speed of TCR-induced signal initiation and the dynamically changing composition of the resulting signaling complexes.

## Results

### Actin-rich protrusions initiate T cell coverslip contacts

T cells engaging TCR-specific stimulatory antibodies on a coverslip establish contact through protruding filopodia and lamellipodia (Bunnell et al., 2001). These contacts trigger dramatic cytoskeletal alterations which result in the spreading of the T cells across the coverslip and the development of a peripheral actin-rich zone (Video 1, available at <http://www.jcb.org/cgi/content/full/jcb.200203043/DC1>). To determine if structures rich in filamentous actin initiate T cell coverslip contacts, we imaged EGFP-actin within the contact while collecting interference reflection microscopy (IRM) images of the contact. As shown in Fig. 1, the tips of projecting lamellipodia (top) are clearly associated with darker structures corresponding to points of close contact (bottom). Thus, actin-dependent protrusive structures may promote the formation of tight contacts between the T cell and coverslip.

### The TCR is specifically clustered within T cell coverslip contacts

To determine whether TCR-dependent signals are initiated in these close contacts, we tracked the sub-cellular localization of the subunits of the TCR. T cells were introduced into chambered stimulatory coverslips, fixed at various times

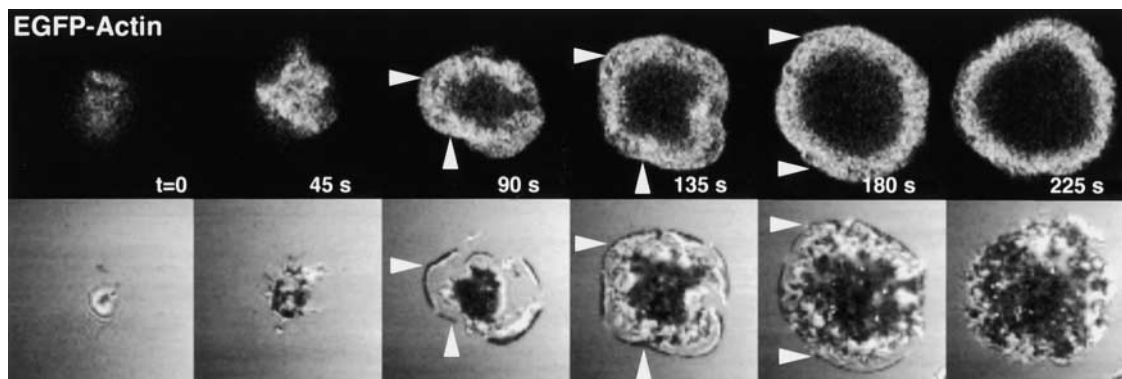
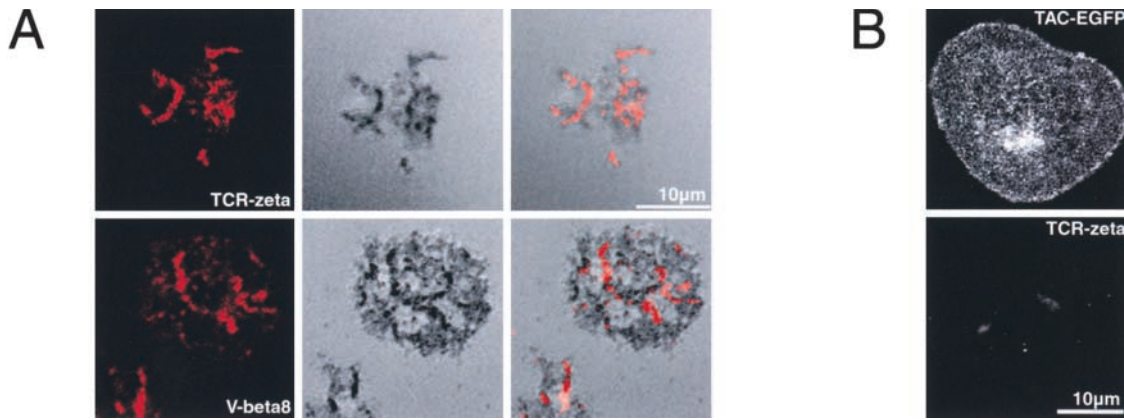


Figure 1. **The rearrangement of the actin cytoskeleton is coupled to contact formation.** Jurkat T cells expressing EGFP-actin were plated on stimulatory coverslips and imaged using a Zeiss LSM 410 confocal system. EGFP-actin and IRM images of the contact were collected every 45 s. Arrowheads emphasize the correspondence between the actin rich structures (top) and the developing contacts (bottom).



**Figure 2. The TCR is specifically clustered within tight contacts.** (A) Jurkat cells were either plated on HIT3a-coated coverslips, fixed after 1 min and stained for TCR $\zeta$  (top), or plated on UCHT1-coated coverslips, fixed after 2 min and stained for V $\beta$ 8 (bottom). Cells were then permeabilized and stained for TCR components (left). Contacts between stained T cells and the coverslip were also imaged by IRM, where tight contacts appear darker than loose contacts (middle). Overlays reveal that receptor engagement occurs preferentially in the zones of tightest contact (right). (B) TAC-EGFP-expressing Jurkat T cells were plated on coverslips and fixed after 5 min. In the top panel, cells were plated on stimulatory HIT3a-coated coverslips and imaged for EGFP. In contrast, in the bottom panel, cells were plated on anti-TAC-coated coverslips and stained for TCR $\zeta$ . No clustering is apparent in either sample.

after plating, and processed for immunofluorescence. TCR $\zeta$  and V $\beta$ 8, the TCR $\beta$  chain present in Jurkat T cells, are observed in clusters 0.5–1.0  $\mu$ m in size shortly after T cell coverslip contact (Fig. 2 A, left). These clusters colocalize with the tight contacts (darker spots) observed by IRM (Fig. 2 A, center and right, overlaid images). Cluster-containing conjugates begin to appear within seconds of plating the T cells onto the coverslip, and the number of detectable clusters in an individual cell reaches a maximum within 3 min, when the T cell coverslip contact reaches its maximum extent (Bunnell et al., 2001). These TCR-containing clusters persist in T cells plated for up to 20 min before fixation (unpublished data). The recruitment of the TCR into these tight contacts is specific, as a control protein composed of the extracellular and transmembrane domains CD25 joined to a cytoplasmic EGFP tag (Tac-EGFP), is not clustered under these conditions (Fig. 2 B, top). Similarly, the recruitment of the TCR into tight contacts requires TCR engagement, as the TCR is not clustered when Tac-EGFP-expressing Jurkat T cells are plated on coverslips coated with antibodies to CD25 (Fig. 2 B, bottom). These observations establish that ligated TCRs are rapidly and specifically clustered in close contacts.

#### Sites of TCR clustering are sites of signal initiation

Next, we tested whether ZAP-70-EGFP was recruited into these TCR-rich clusters. Like the TCR, ZAP-70 is recruited into clusters that coincide with contact sites (Fig. 3 A; Video 2, available at <http://www.jcb.org/cgi/content/full/jcb.200203043/DC1>). This process is extremely rapid, and occurs within 15 s of the initial formation of a contact. The immature contacts into which ZAP-70 is initially recruited are the size of individual TCR-rich clusters (Fig. 3 A, top row, left; note the contact marked by the white arrowhead). The formation of new ZAP-70-containing clusters continues until the contact reaches its maximum extent,  $\sim$ 3 min into the spreading process (Video 2). TCR-induced tyrosine phosphorylation parallels the spreading process. Phosphoty-

rosine is detectable within 30 s of the initiation of these assays (unpublished data), and reaches a maximum after  $\sim$ 3 min (Fig. S1). These observations suggest that PTK-dependent signals are initiated in newly formed TCR clusters. To confirm the tyrosine phosphorylation of critical signaling molecules in these tight contacts, we imaged ZAP-70-EGFP, phosphotyrosine, and TCR $\zeta$  in T cell coverslip contacts (Fig. 3 B). As expected, the ZAP-70 clusters (green) colocalized extensively with the clusters of TCR $\zeta$  (red). Phosphotyrosine-containing proteins (blue) were specifically observed in regions of extensive colocalization between TCR $\zeta$  and ZAP-70 (compare overlays 1 and 2). Therefore, PTK-dependent signal transduction is initiated in TCR-rich clusters closely apposed to the stimulatory coverslip. Treatment with PP2, an inhibitor of Lck and Fyn, drastically reduces total tyrosine phosphorylation and prevents the recruitment of ZAP-70 into TCR-containing clusters without inhibiting the clustering of the TCR itself (Fig. 3 C). Thus, the organization of the TCR into clusters precedes the tyrosine phosphorylation required for the initiation of downstream signals.

#### Signaling adapters and effectors are selectively recruited to phosphotyrosine-rich signaling assemblies

To test whether the adapters and effectors required for downstream signal transduction are also recruited into signaling clusters, we examined T cells fixed 2 min after plating. Due to delays in the settling of the cells onto the stimulatory coverslips, the cells shown here have been spreading for 1 to 2 min. Two representative cases are shown in Fig. 4, where ZAP-70 and Grb2 (left), and LAT and Gads (right) colocalized with one another in clusters within tight contacts (dark points). More extensive studies have shown that ZAP-70, LAT, Grb2, Gads, SLP-76, and Cbl all transiently colocalize in TCR-containing, phosphotyrosine-rich signaling complexes tightly associated with the stimulatory coverslip (Fig. S2; unpublished data). Several control surface proteins fail to accumulate in the clusters (Fig. S2). Tac-EGFP neither accumulated in nor was excluded from the signaling

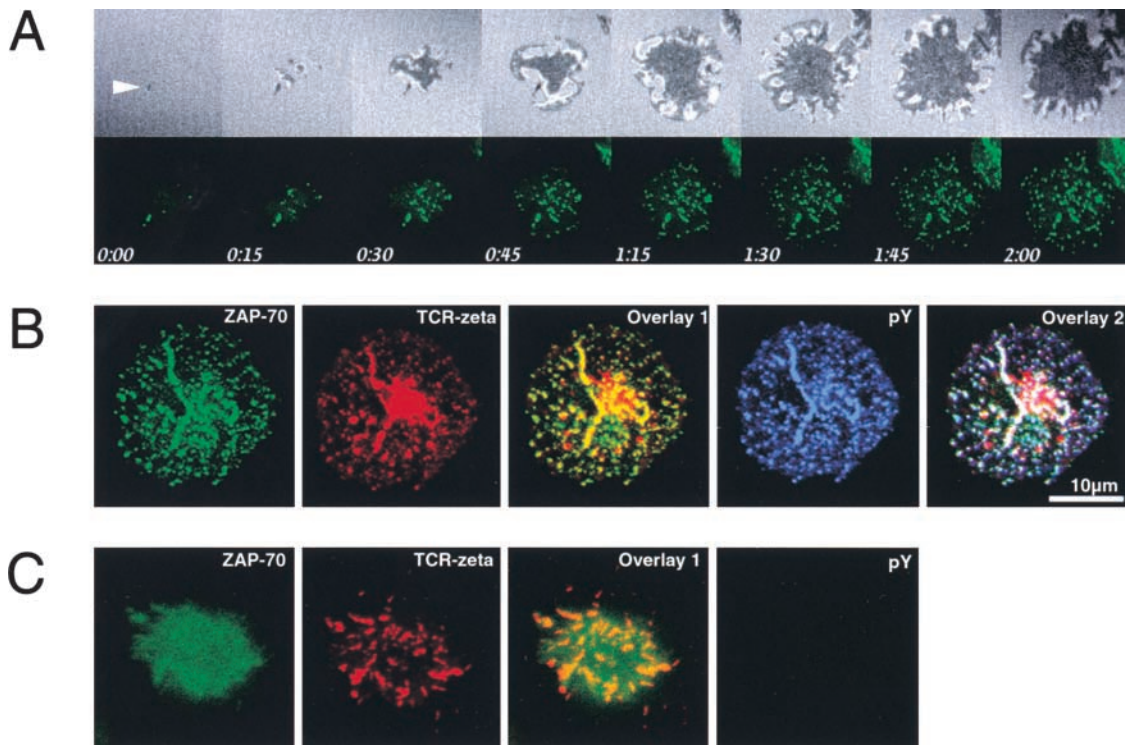


**Figure 3. ZAP-70 is specifically recruited to activated TCRs in tight contacts.** (A) Jurkat T cells expressing ZAP-70-EGFP were plated on coverslips. ZAP-70-EGFP and IRM images were collected every 15 s using the Zeiss LSM 410. The white arrow marks the earliest observed signaling cluster and contact point. (B) Jurkat T cells expressing ZAP-70-EGFP were plated on stimulatory coverslips, fixed after 5 min, and stained for both TCR $\zeta$  and phosphotyrosine. ZAP-70-EGFP, TCR $\zeta$ , and phosphotyrosine were pseudocolored green, red, and blue, respectively. The TCR $\zeta$  staining pattern shows a large cluster in the center of the contact; this strong signal results from the staining of a large, perinuclear pool of TCR $\zeta$ . (C) Cells were processed and imaged as in B after pretreatment and stimulation in the presence of 10  $\mu$ M PP2.

complexes. In contrast, CD43 was excluded from the entire contact interface, and CD45 was specifically excluded from ZAP-70-rich signaling clusters. These studies demonstrate that TCR-containing signaling assemblies form at sites of close contact between the T cell and coverslip and that adapters critical to T cell activation are recruited to these assemblies quickly and specifically.

#### Contacts the size of individual clusters are sufficient to initiate calcium influxes

To determine whether these signaling assemblies could induce calcium elevations, we monitored contact formation and intracellular calcium levels in parallel. Two representa-

tive cells are shown in Fig. 5, A and B. Here, intracellular calcium levels in the responding cells jump from low (blue) to high (red) levels within 24 s. In fact, as shown in the corresponding movies and calcium traces (Fig. 5, C and D; Videos 3 and 4, available at <http://www.jcb.org/cgi/content/full/jcb.200203043/DC1>), calcium levels frequently go from basal to maximal levels within one frame, or 12 s. These calcium elevations are typically triggered in response to the formation of one or two point contacts the size of individual signaling clusters (Fig. 5, A and B, white arrows). During the subsequent spreading response, continued oscillations in intracellular calcium were observed. These results suggest that biochemically competent signal-

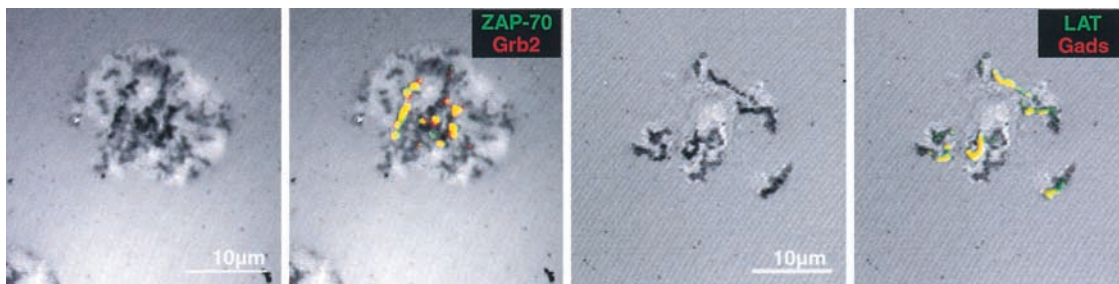


**Figure 4. Signal transducing complexes form at tight contacts.** Jurkat T cells stably expressing either ZAP-EGFP or LAT-EGFP (green) were plated on stimulatory coverslips, fixed after 2 min, permeabilized, and stained for either Grb2 or Gads (red). IRM images (left) and fluorescent overlays on the IRM images (right) are shown. Note the strong correspondence between tight contacts and clusters of signaling proteins.

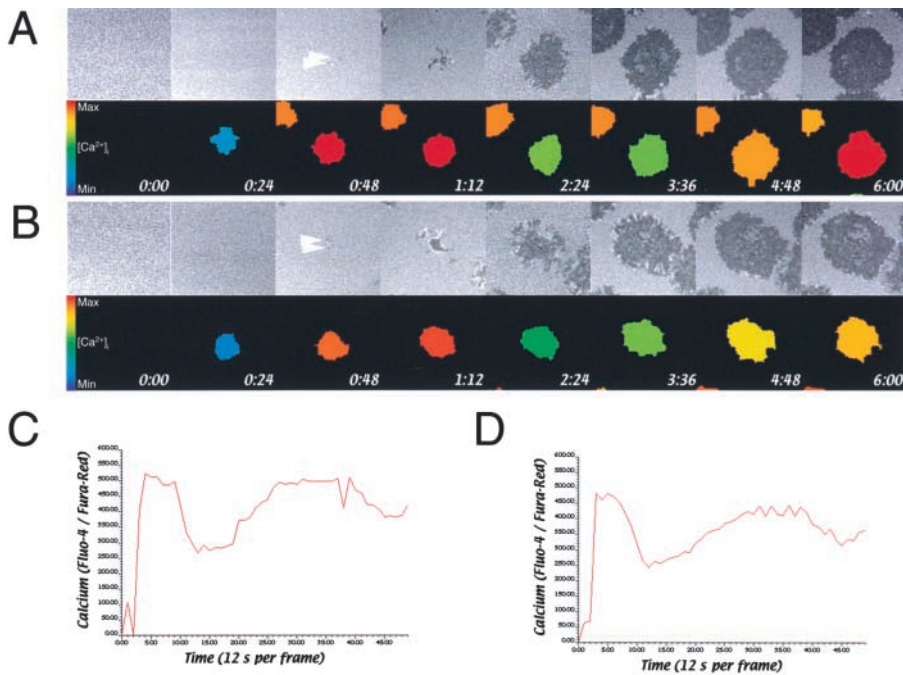


**Figure 5. Small contacts are sufficient to initiate calcium influxes.**

(A and B) Jurkat T cells loaded with the calcium responsive dyes Fluo-4 and Fura-Red were plated on coverslips and dynamically imaged for calcium content and T cell-coverslip contact. In the bottom panels the bodies of responding T cells are pseudocolored to indicate their calcium content. The pseudocolored calcium scale is inset in the leftmost panels. White arrows mark the earliest observed contact points. (C and D) Traces of calcium over time for the two cells shown in A and B. The time axis is marked in frames; one frame corresponds to 12 s. These traces are representative of those obtained from >30 cells imaged in three separate experiments.

ing complexes can be assembled quickly within individual point contacts.

### Cluster components exhibit distinct patterns of movement

To dynamically observe the formation and dissipation of these signaling assemblies, we tracked the redistribution of individual chimeric signaling proteins during T cell spreading and activation. ZAP-70-EGFP is present in clusters which are stable over time (Fig. 6 A; Video 5, available at <http://www.jcb.org/cgi/content/full/jcb.200203043/DC1>). Studies carried to later timepoints demonstrate that clusters containing ZAP-70 persist for at least 20 min without moving laterally (unpublished data). Quantitative analyses show that ZAP-70 is incorporated into clusters forming near the leading edge of the contact (Fig. S3). LAT and Grb2 are incorporated into clusters in a similar manner and with similar kinetics. In contrast to ZAP-70, LAT-EGFP gradually disappears from the contact over 2 to 3 min (Fig. 6 B; Video 6, available at <http://www.jcb.org/cgi/content/full/jcb.200203043/DC1>). Although the mechanisms governing the exit of LAT remain obscure, LAT may leave these signaling complexes in small vesicular intermediates (Video 6). Grb2-containing clusters also persist for ~2 to 3 min before fading from the contact (Fig. 6 C; Video 7, available at <http://www.jcb.org/cgi/content/full/jcb.200203043/DC1>). Enhanced green fluorescent protein (EYFP)-Gads is also recruited to the T cell coverslip contact, where it forms clusters that persist for no more than 1 min (Fig. 6 D; Video 8, available at <http://www.jcb.org/cgi/content/full/jcb.200203043/DC1>). In contrast, SLP-76-EYFP behaves uniquely. After its rapid recruitment into clusters, SLP-76 translocates towards the center of the contact in large cohesive structures (Fig. 6 E; Video 9, available at <http://www.jcb.org/cgi/content/full/jcb.200203043/DC1>). This pattern of movement results in the accumulation of SLP-76

in the center of the contact, near the coverslip. Therefore, although signaling molecules are coordinately recruited into signaling assemblies at the leading edges of contacts, these proteins depart by distinct mechanisms.

### ZAP-70 initially equilibrates between signaling complexes

As shown above, signaling clusters containing ZAP-70 are laterally immobile within the plane of the coverslip. To test whether or not individual ZAP-70 molecules are stably bound to these immobile clusters, we monitored fluorescence recovery in photobleached and control regions. The recovery of fluorescence in the bleached region was rapid and nearly complete when the responding cells had been plated for 2 min before bleaching (Fig. 7 A, red box; Video 10, available at <http://www.jcb.org/cgi/content/full/jcb.200203043/DC1>). The recovered fluorescence retained the pattern of clustering observed prior to the bleach, indicating that ZAP-70 equilibrates freely between bleached complexes and an unbleached pool of ZAP-70 elsewhere in the cell. The recovery of fluorescence in older complexes, present in cells plated for 20 min before bleaching, was much less complete (Fig. 7 B, red box; Video 11, available at <http://www.jcb.org/cgi/content/full/jcb.200203043/DC1>). The same trends can be observed in plots showing the recovery of fluorescence after bleaching (Fig. 7, C and D). The extent of fluorescence recovery drops with increasing time of plating, as shown in Fig. 7 E. Nevertheless, the time to half-maximal fluorescence recovery is independent of the time at which the cells are bleached, and remains between 7.5 and 10 s (Fig. 7 E). Therefore, although ZAP-70-containing clusters appear to be static, these clusters rapidly exchange ZAP-70 molecules for several minutes. At present, we do not know whether additional cluster components equilibrate in this manner; these studies have been hindered by the transient nature of the clustering displayed by LAT, Grb2, and Gads.

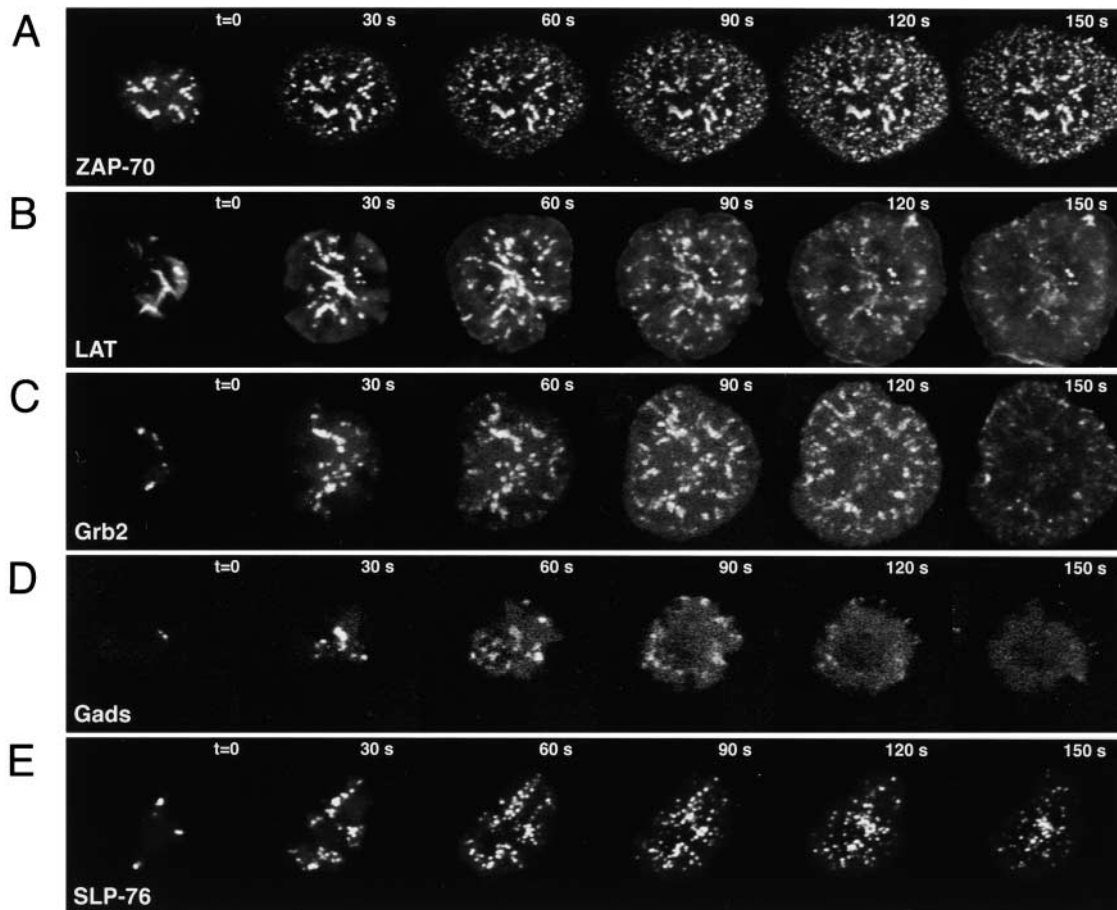


Figure 6. **Signaling adaptors are dynamically redistributed throughout contact formation.** (A–E) Live Jurkat E6.1 cells expressing EGFP- or EYFP-chimeras were plated on stimulatory coverslips and observed dynamically using the Ultraview spinning wheel confocal system. Seven-image, 3.5  $\mu\text{m}$  deep Z stacks were collected every 10 s for ZAP-70, every 15 s for the remaining proteins.

### A nonphosphorylated lipid raft marker is not retained in signaling complexes

Several reports have suggested that TCR ligation results in the coordinated accumulation of lipid rafts with the aggregated TCR (Janes et al., 1999). As a lipid raft component, LAT could be passively stabilized in signaling complexes through interactions with rafts associated with the activated TCR. To test this hypothesis we tracked the localization of LAT-EGFP and EYFP-GPI, a lipid raft marker (Keller et al., 2001). As shown above, LAT-EGFP transiently clusters upon T cell activation (Fig. 8 A; Video 12, available at <http://www.jcb.org/cgi/content/full/jcb.200203043/DC1>). In contrast, EYFP-GPI does not cluster in this manner, suggesting that raft association is insufficient to direct clustering (Fig. 8 B; Video 13, available at <http://www.jcb.org/cgi/content/full/jcb.200203043/DC1>). Fixed cell studies confirmed that LAT accumulates within signaling clusters identified by immunofluorescent staining for phosphotyrosine (Fig. 8 C). YFP-GPI, in contrast, does not colocalize with these signaling clusters, and appears to form aggregates alongside the phosphotyrosine-rich signaling clusters (Fig. 8 D). These data indicate that lipid raft components do not nonspecifically accumulate in signaling clusters. Furthermore, the inhibition of Src-family kinases by PP2 revealed that the clustering of LAT is strictly tyrosine kinase-depend-

ent (Fig. 8, E and F). These data indicate that the accumulation of LAT in signaling clusters is unlikely to be stabilized solely through interactions with lipid rafts, but does require phosphotyrosine-dependent interactions.

### Characterizing the formation and movement of SLP-76-rich structures

To demonstrate that the unique movement of SLP-76 requires activation of the TCR, we plated SLP-76-YFP-expressing cells on coverslips coated with nonstimulatory antibodies. SLP-76 is recruited into moving clusters in response to TCR-ligation (see above; Fig. 9 A; Video 14, available at <http://www.jcb.org/cgi/content/full/jcb.200203043/DC1>), but not in response to either CD45 (Fig. 9 B; Video 15, available at <http://www.jcb.org/cgi/content/full/jcb.200203043/DC1>) or CD43 ligation (Fig. 9 C; Video 16, available at <http://www.jcb.org/cgi/content/full/jcb.200203043/DC1>). Furthermore, resting SLP-76-YFP-expressing cells contain few or no detectable vesicle-like accumulations of SLP-76 (unpublished data). One property of the movement of SLP-76-rich structures observed in Videos 9 and 14 is striking: entire SLP-76-containing clusters arising at the periphery of the contact translocate radially towards the center of the contact within 1 to 2 min of their formation. This centrally directed movement is inhibited by

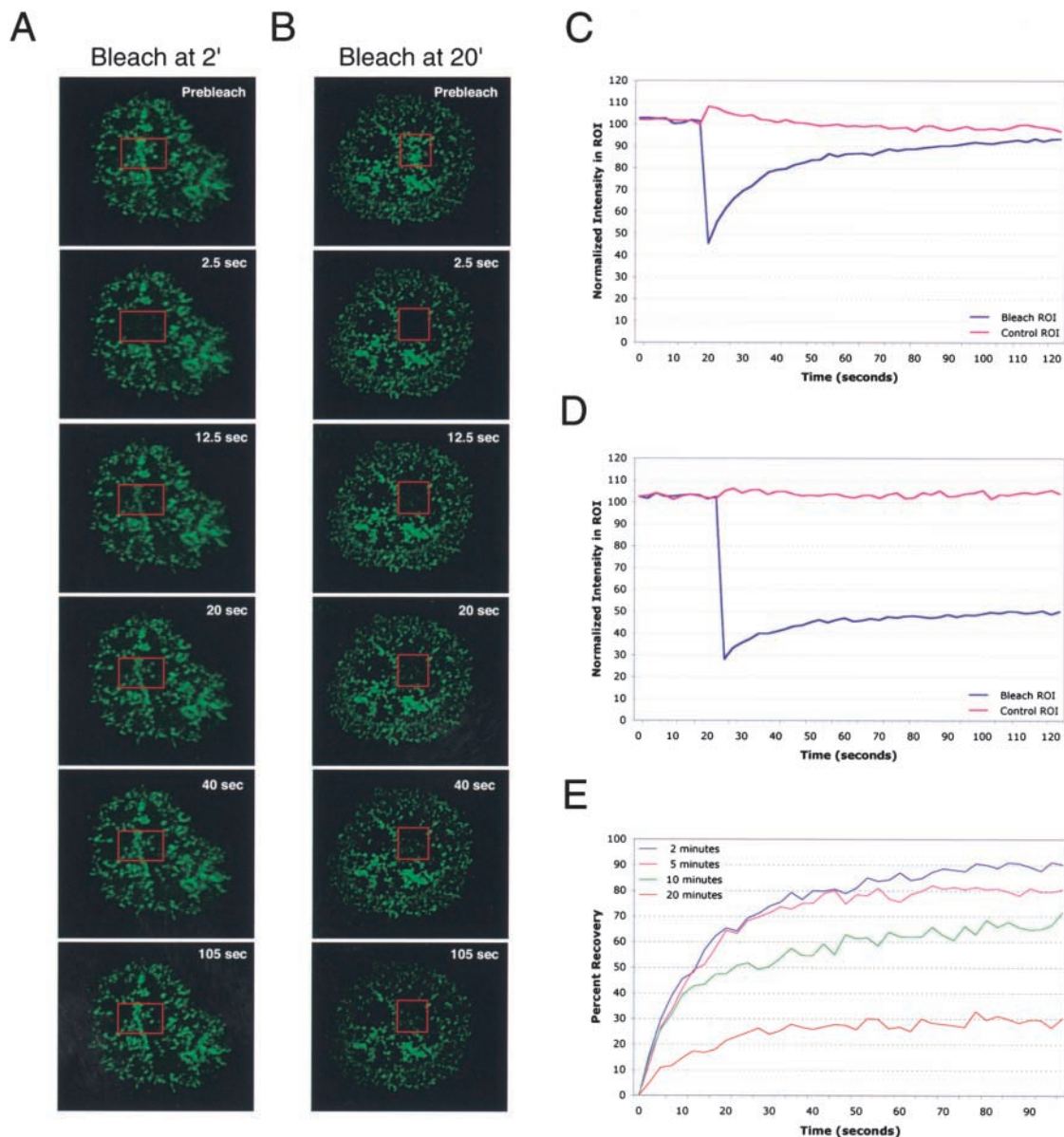


Figure 7. **Photobleaching reveals that ZAP-70 equilibrates between signaling complexes.** (A and B) ZAP-70-EGFP-expressing Jurkat T cells were plated on coverslips and allowed to develop contacts for either 2 or 20 min. Contacts were imaged for 20 s, photobleached within a specific region of interest (ROI, red boxes), and monitored for the recovery of fluorescence in the bleached ROI. Images were obtained every 2.5 s. (C) Mean fluorescence recovery traces from cells plated for 2 min before photobleaching ( $n = 6$ ). (D) Mean fluorescence recovery traces from cells plated for 20 min before photobleaching ( $n = 6$ ). (E) The extent of fluorescence recovery in bleached ROIs as a function of the age of the observed contacts at the time of photobleaching. In each case, half-maximal recovery is observed within 7.5 to 10 s.

colchicine treatment, and is therefore dependent on the microtubule cytoskeleton (Fig. 10, A and B; Movies 17 and 18, available at <http://www.jcb.org/cgi/content/full/jcb.200203043/DC1>). Although several vesicular compartments display directed movement along microtubules, we have not yet been able to conclusively identify SLP-76-containing structures with any known intracellular compartments. As shown in Fig. 10 C, SLP-76 does not colocalize with transferrin, a marker of the endosomal recycling pathway (Video 19, available at <http://www.jcb.org/cgi/content/full/jcb.200203043/DC1>); EEA1, a marker of early endosomes; Rab11, a marker of recycling endosomes; or TGN46, a marker for the trans-Golgi network (Hopkins and Trow-

bridge, 1983; Gruenberg and Maxfield, 1995; Mu et al., 1995; Ullrich et al., 1996; Prescott et al., 1997). SLP-76 also failed to colocalize with GM130, a marker for the stacks of the Golgi apparatus (unpublished data; Nakamura et al., 1997). The identification of the SLP-76-containing compartment is obviously of significant interest, but will require further study.

## Discussion

### The visualization of signaling complexes in live T cells

To date, microscopic studies of live T cells undergoing activation have primarily focused on the movements of

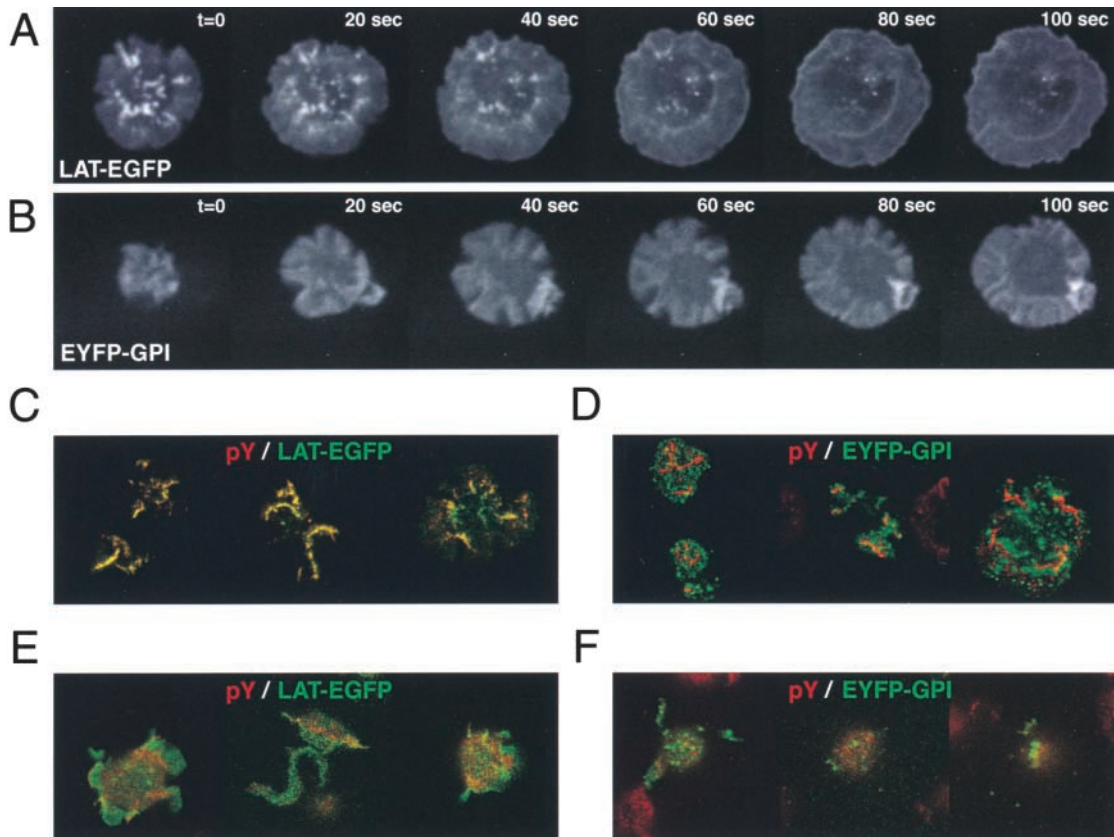


Figure 8. **LAT is selectively retained in signaling complexes.** (A and B) Jurkat cells expressing either LAT-EGFP or EYFP-GPI were plated on stimulatory coverslips and imaged using the Ultraview system. Five-image, 2.5  $\mu\text{m}$  deep Z stacks were collected every 20 s. The bright spot observed in the EYFP-GPI-expressing cells corresponds to a membrane fold, not a cluster. Similar structures are also occasionally observed with Tac-EGFP, a nonraft membrane protein. (C and D) Jurkat cells expressing either LAT-EGFP or EYFP-GPI (green) were plated on stimulatory coverslips, fixed after 2 min, and stained for phosphotyrosine (red). (E and F) Jurkat cells expressing either LAT-EGFP or EYFP-GPI were treated with 10  $\mu\text{M}$  PP2, and then plated and imaged in C and D.

the transmembrane proteins that define the immunological synapse (TCR, CD4, CD28, LFA-1, CD43, CD45) (Monks et al., 1998; Grakoui et al., 1999; Dustin and Cooper, 2000; Johnson et al., 2000; Krummel et al., 2000; Al-

lenspach et al., 2001; Delon et al., 2001; Lee et al., 2002; Zal et al., 2002). With the exception of Lck, little is known about the movements of proteins recruited to signaling complexes in response to receptor engagement (Richie et

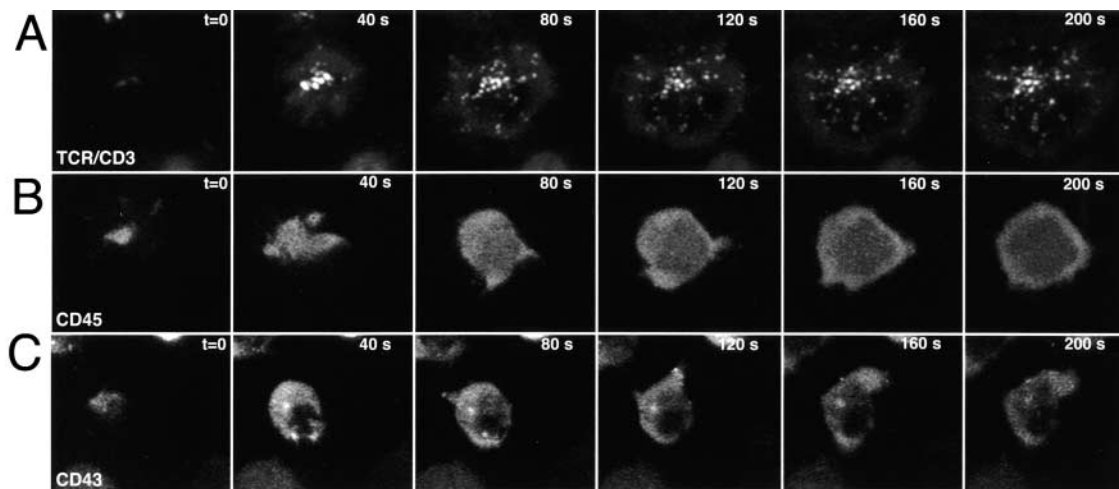


Figure 9. **SLP-76 clustering is selectively induced by TCR ligation.** (A and C) SLP-76-EYFP expressing J14 cells were plated on antibody-coated coverslips and imaged using the Ultraview system. Five-image, 2.5  $\mu\text{m}$  deep Z stacks were collected every 10 s. The plate-bound antibodies were specific for (A) CD3 $\epsilon$ , (B) CD45, or (C) CD43.

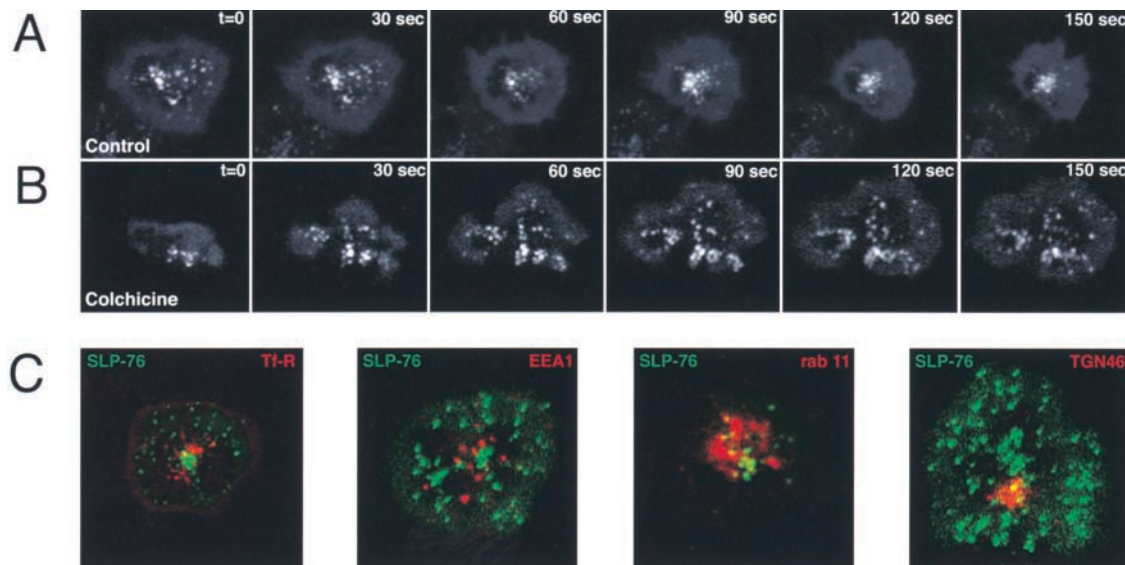


Figure 10. **SLP-76-containing clusters move on microtubules to an undefined perinuclear compartment.** (A and B) Jurkat J14 cells expressing SLP-76–EYFP were plated on stimulatory coverslips and imaged as in Fig. 9 after 1 h pretreatment with either DMSO carrier (A) or 100  $\mu$ M colchicine (B). Drugs were also present throughout imaging. (C) The colocalization of SLP-76–EYFP with various intracellular markers was tested in both live and fixed cells. Jurkat J14 cells expressing SLP-EGFP (green) were serum starved for 40 min, incubated with 100  $\mu$ M transferrin-Alexa 594 (red), plated on stimulatory coverslips and imaged using the Ultraview system. Every 20 s, individual red and green image stacks were collected. Each image stack is five images (2.5  $\mu$ m) deep. The image shown here was collected 2 min into the spreading process (panel 1). Jurkat J14 cells expressing SLP-76–EYFP (green) were also plated on stimulatory coverslips, fixed after 10 min, and stained for intracellular markers (red): (panel 2) EEA1; (panel 3) rab11; or (panel 4) TGN46.

al., 2002). Using a novel assay system, we have monitored the dynamic redistribution of ZAP-70, LAT, Grb2, Gads, and SLP-76 in response to TCR ligation, significantly extending the number of intracellular signaling molecules studied in living T cells. In this manner, we have observed the formation of tyrosine-phosphorylated signaling complexes 0.5–1.0  $\mu$ m in size and enriched in the TCR, ZAP-70, LAT, Grb2, Gads, SLP-76, and Cbl. These signaling clusters develop rapidly within domains of the plasma membrane tightly associated with the stimulatory coverslip and are individually competent to induce intracellular calcium elevations. Strikingly, these structures are continuously assembled and disassembled throughout the process of contact formation. Finally, we have shown that recruited molecules depart from these signaling complexes by distinct mechanisms. SLP-76, in particular, exits the TCR-rich clusters in a unique manner that suggests an ongoing role in signal transduction.

### The assembly of TCR-containing complexes

The most critical event in the initiation of antigen receptor-dependent signaling in T cells is the aggregation of the TCR (Boniface et al., 1998). In our system, the TCR is recruited into clusters even though the TCR-specific stimulatory antibodies we use are uniformly distributed across our coverslips (unpublished data). The clustering of the TCR is PP2-insensitive, and is therefore independent of downstream PTK-driven signaling pathways. Strikingly, TCR-rich clusters preferentially form in membrane domains tightly apposed to the stimulatory coverslip. These observations are consistent with models of immune synapse formation in which the TCR is preferentially engaged within membrane do-

main separated by a narrow gap compatible with TCR-ligand engagement (Shaw and Dustin, 1997; Anton van der Merwe et al., 2000). Because we rarely observe TCR-rich clusters that are not tyrosine phosphorylated, PTK-dependent phosphorylation must be rapidly triggered after the clustering of the TCR. ZAP-70, which binds directly to the signal-transducing subunits of the TCR upon their phosphorylation, is recruited into clusters within 6–15 s of contact initiation, supporting this conclusion. As expected, the clustering of ZAP-70 is sensitive to PP2. Thus, the formation of functional signaling complexes requires phosphotyrosine-dependent interactions, whereas the initial clustering of the TCR does not.

### The assembly of LAT-nucleated complexes

LAT nucleates the formation of signaling complexes critical to T cell activation. Our live-cell studies have shown that LAT is specifically recruited into clusters within 15 s of TCR ligation. Several components of the LAT-nucleated complex, including Grb2, Gads, and SLP-76, are recruited into clusters within a similar time frame. Furthermore, our fixed cell studies have shown these LAT-containing complexes are coincident with the ZAP-70-containing clusters described above. This observation confirms that ZAP-70 is poised to phosphorylate two of its most prominent substrates, LAT and SLP-76, in intact T cells. Previously, these interactions had only been observed in purified membranes (Harder and Kuhn, 2000; Wilson et al., 2001).

### Lipid rafts and complex assembly

Normal T cell activation requires the association of LAT with lipid rafts (Zhang et al., 1998b). Because lipid

raft components have been reported to accumulate with crosslinked antigen receptors, TCR ligation may govern the clustering of LAT by directing the local accumulation of lipid rafts (Xavier et al., 1998; Janes et al., 1999; Hollowka et al., 2000). However, the extensive accumulation of lipid rafts at sites of receptor ligation does not appear to be an essential prerequisite of T cell activation. For example, Th2 cells responding to antigen-loaded APCs do not significantly accumulate lipid raft components in their contacts (Balamuth et al., 2001). Additionally, the direct crosslinking of the TCR at 37°C does not necessarily result in the enrichment of either cholesterol or GM1 in receptor-associated membranes (Harder and Kuhn, 2000). Here, we were unable to observe the recruitment of a lipid raft marker, EYFP-GPI, into signaling clusters. Therefore, interactions between LAT and receptor-associated raft components are unlikely to explain the clustering of LAT with the TCR. In contrast, the recruitment of LAT into clusters is PP2-sensitive, indicating that PTK-dependent scaffolds play a dominant role in the clustering of LAT. Nevertheless, lipid rafts could be required for the initiation, rather than the maintenance, of interactions between LAT and TCR-associated signaling proteins. Given the basal association of LAT with lipid rafts, these observations suggest that LAT is either abstracted from lipid rafts during cluster formation, or present in a subset of lipid rafts distinct from that containing EYFP-GPI. The induced segregation of LAT from other lipid raft components could contribute to T cell activation by limiting the recruitment of lipid raft-associated negative regulators of activation, such as Cbp/PAG, to the TCR (Brdicka et al., 2000; Kawabuchi et al., 2000).

### Signal initiation by minimal complexes

Calcium elevations typically begin within 12 s of contact initiation, when the T cell coverslip contact consists of a few small points. This lag between the initiation of contact and the elevation of calcium is similar to the time required for complex formation. Because the point contacts present at this time are the size of a single TCR-rich cluster the minimal functional unit required for calcium elevations may be a single cluster. The early onset of these calcium elevations is consistent with the permissive role of intracellular calcium in T cell spreading (Bunnell et al., 2001). Strikingly, this behavior parallels that of T cells engaging APCs, which also elevate intracellular calcium before initiating more active contact with their targets, but do so after a variable lag which may correspond to the time required to form a single functional signaling complex (Negulescu et al., 1996; Delon et al., 1998).

### The dynamic composition of signaling complexes

Signaling complexes quickly disassemble, reassemble, and change in composition as specific proteins dissociate. ZAP-70 achieves a steady state where it remains associated with laterally immobile clusters for 30 min or more. In contrast, LAT, Grb2, Gads, and SLP-76 are transiently recruited to signaling complexes, and disappear from these structures within 1–3 min. Our FRAP studies have shown that early in the spreading process ZAP-70, which appears to be im-

mobile, disassociates from and reassociates with signaling complexes quickly enough to half maximally repopulate bleached complexes within 7.5–10 s. This rate of recovery is consistent with that observed in a previous FRAP study that examined the reassociation of ZAP-70 with the activated TCR in a non-T cell model (Sloan-Lancaster et al., 1998). Cells bleached later in the spreading process displayed similar rates of fluorescence recovery, but recovered to a lesser extent. Because the rate of recovery remains constant, the dissociation and reassociation rates are probably unchanged at these later timepoints. The reduced extent of fluorescence recovery could be explained by three mechanisms: TCRs are rendered incapable of rebinding ZAP-70, free ZAP-70 becomes incapable of rebinding the TCR, or existing receptor-kinase complexes are prohibited from dissociating. Because the kinetics with which fluorescence recovery declines are similar to the kinetics with which receptor phosphorylation is lost, the time-dependent reduction in fluorescence recovery may be caused by the dephosphorylation of the TCR.

### Signaling complexes as protosynapses

Multiple signals are triggered by TCR engagement prior to the formation of a central TCR-rich cluster, or cSMAC (Negulescu et al., 1996; Delon et al., 1998; Grakoui et al., 1999; Lee et al., 2002). These signals may be initiated by TCR-rich clusters, or protosynapses, that develop in advance of the mature cSMAC (Grakoui et al., 1999; Dustin and Cooper, 2000; Krummel et al., 2000). The TCR-rich clusters observed here resemble these protosynapses in several respects, including their size, kinetics of formation, and ability to exclude CD43 and CD45 (Sperling et al., 1998; Johnson et al., 2000). Although interactions between engaged TCRs and coverslip-bound stimulatory antibodies preclude the translocation of TCRs into a central cluster, we observe most of the biochemical outputs induced by antigen-loaded APCs. Our results suggest that protosynapses are capable of directing T cell activation in the absence of cSMAC formation and could drive the activation of thymocytes and Th2 cells, which do not form well-defined SMACs (Balamuth et al., 2001; Richie et al., 2002). We also observed the continuous dissociation of components from these signaling complexes, suggesting that the generation of new complexes throughout contact formation is required to maintain the levels of tyrosine phosphorylation observed when T cell contacts and synapses reach their greatest extent (Lee et al., 2002). In addition, the formation of these new clusters at the leading edge may facilitate the coupling of the TCR to the active remodeling of the actin cytoskeleton through downstream adaptors, such as SLP-76 (Krause et al., 2000).

### Molecular fates postclustering

The molecular clusters observed here function as both signaling and sorting structures. These complexes are assembled from proteins residing in multiple cellular compartments. ZAP-70 remains associated with signaling complexes, LAT departs the complexes by undefined mechanisms, and both Grb2 and Gads dissociate into the cytosol. In contrast, SLP-76 departs TCR-rich signaling com-

plexes in large structures specifically induced by TCR ligation. These structures are transported along microtubules as discrete units and accumulate in an undefined perinuclear structure not labeled with markers specific for early endosomes, recycling endosomes, the Golgi apparatus, or the TGN. The association of SLP-76 with these structures persists to timepoints at which neither clusters of Grb2 nor Gads can be detected. Although amounts of LAT and Gads beneath the threshold for visualization may direct the movement and localization of SLP-76, we believe that SLP-76 dissociates from LAT-nucleated complexes and enters these novel structures by a distinct and as of yet undefined mechanism.

### Potential consequences of late trafficking events

The termination of signal transduction through the targeting of signaling molecules into degradative compartments has been well described (Strous and Govers, 1999). In non-T cells, internalization has also been shown to direct signaling molecules into intracellular compartments from which they can initiate novel signals (Daaka et al., 1998). The consequences of the protein trafficking described here are not yet clear. The sustained recruitment of SLP-76 to a perinuclear vesicular compartment might in some way contribute to T cell activation. Many questions remain regarding the functional consequences of these molecular sorting events and the identities of the structures that contain sorted signaling molecules. In future studies we will image the redistribution of multiple chimeric proteins, lipid markers, and labeled proteins during T cell activation, helping to resolve these issues.

## Materials and methods

### Materials

The CD3 $\epsilon$ -specific monoclonal antibodies used to induce T cell spreading (HIT3a and UCHT1) were obtained from Pharmingen. Anti-CD25 (anti-TAC) was obtained from UBI. Primary staining antibodies were from the following suppliers: V $\beta$ 8, CD43, and CD45 were from Pharmingen; Gads and phosphotyrosine (4G.10) were from UBI; TCR $\zeta$ , and Cbl were from Santa Cruz Biotechnology, Inc.; SLP-76 was from Antibody Solutions; and Grb2, EEA1, Rab11, TGN46, and GP130 were from Transduction Labs. Alexa-conjugated isotype-specific secondary antibodies, Alexa-conjugated transferrin, Fluo-4, and Fura-Red were purchased from Molecular Probes. The expression vectors pEGFP-n1, pEYFP-n1, and pEYFP-c3 were obtained from CLONTECH Laboratories, Inc. The SLP-76-deficient Jurkat T cell line J14 was provided by Arthur Weiss (University of California San Francisco, San Francisco, CA). RPMI 1640 and G418 were obtained from GIBCO BRL. All other tissue culture supplies were from Biofluids. All remaining chemicals are from Sigma-Aldrich. Jurkat T cells and derivatives were maintained as described previously (Bunnell et al., 2001).

### Constructs and the generation of stable cell lines

The ZAP-70-EGFP, Grb2-EYFP, and EYFP-GL-GPI chimeras have been described (Sloan-Lancaster et al., 1998; Keller et al., 2001; Yamazaki et al., 2002). The TAC-EGFP chimera was provided by Dr. J. Donaldson (National Institutes of Health, Bethesda, MD). The remaining chimeric proteins were derived by standard methods. All chimeras were fully functional, as assessed by biochemical complex formation, and, where possible, by the reconstitution of deficient cell lines. Jurkat E6.1 cells stably expressing EGFP-actin have been described. Jurkat E6.1 cells expressing either TAC-EGFP, ZAP-70-EGFP, LAT-EGFP, Grb2-EYFP, or EYFP-Gads, and J14 cells expressing SLP-76-EYFP were generated as described (Bunnell et al., 2001). The stable lines used in these studies express the chimeric signaling proteins at approximately physiological levels. EYFP-GL-GPI was transiently transfected into Jurkat E6.1 cells using the AMAXA electroporation system.

### Spreading assays

Spreading assays were performed as described, with the following modifications for either immunofluorescent staining or for biochemical analyses (Bunnell et al., 2001). For inhibitor studies, cells were preincubated with the corresponding drugs for 1 h, and then plated and imaged in the presence of the drug. For staining procedures, four-chambered coverglasses (Lab-Tek II; Nunc/Nalgene) were coated with either UCHT1 or HIT3a, as required, warmed, and preloaded with 300  $\mu$ l/ml of normal culture media supplemented with 25 mM Hepes. Cells ( $2 \times 10^5$ ) were injected into the bottoms of the chambers in 100  $\mu$ l of normal media and fixed at the indicated times by the addition of 600  $\mu$ l 4% paraformaldehyde in PBS. After 30 min of fixation at 37°C, the chambers were rinsed three times in PFN buffer (PBS, 10% FBS, and 0.02% sodium azide), permeabilized for 5 min with 0.1% Triton X-100 in PBS, rinsed three times in PFN, and blocked for 1 h in PFN-G (PFN supplemented with 2% normal goat serum). Blocked chambers were incubated for 1 h with the indicated primary antibodies diluted in PFN-G, rinsed three times in PFN, and stained for 1 h with isotype-specific Alexa-conjugated goat antisera diluted in PFN-G. Stained cells were rinsed three times in PBS and imaged as below. For the immunofluorescent visualization of TCR subunits cells were fixed in a final paraformaldehyde concentration of 0.25% and 500  $\mu$ g/ml digitonin was used for permeabilization.

### Cellular imaging

All IRM and corresponding fluorescent images were collected on a Zeiss LSM 410 confocal microscope, as described (Bunnell et al., 2001). Ratio-metric calcium measurements correlated with IRM images were collected by alternately visualizing Fluo-4 and Fura-Red in the cell body with a wide pinhole, and taking images of the contact interface under normal conditions. Jurkat E6.1 cells were loaded with calcium indicators, as described, and maintained in the presence of 0.5 mM probenecid (Liu et al., 1998; Jung et al., 2001). The dynamic rearrangements of the actin cytoskeleton and of chimeric signaling molecules during spreading responses were monitored using a Perkin-Elmer Ultraview spinning wheel confocal system equipped with an Orca-ERII CCD camera (Hamamatsu), and filters suitable for the visualization of both EGFP and red dyes. For these live studies, samples were illuminated with either the 488- or 568-nm laser lines from a krypton/argon laser. Live images were collected as vertical Z-stacks which were projected in three dimensions or subsampled for the plane of the coverslip. All photobleaching studies were performed using a Zeiss LSM 510. Cells were imaged for 20 s, photobleached within a specific region of interest (ROI) using the combined 458- and 488-nm laser lines, and then imaged over time. All images were collected using a 63 $\times$  Plan-Apochromat objective (Carl Zeiss). For live studies, the temperature of the sample was maintained at 37°C using a hot air blower (Nevtek) and an objective heater (Bioptechs).

### Image processing and quantitation

IP Lab 3.5 was used for most image processing. Adobe Photoshop (v. 5.0) was used to prepare composite images and for all annotations. Calculations for the photobleaching studies were performed in Excel. Mean fluorescence recovery traces were calculated by monitoring fluorescence intensity over time in the bleached region and in a control region containing similar total fluorescence, normalizing fluorescence in these regions by the total cell fluorescence; and setting the normalized fluorescence during the prebleach interval to 100% before averaging. The percent recovery of fluorescence in bleached regions is calculated by taking the differential between the normalized mean fluorescence intensities within the control and bleached regions, and scaling so that the maximum differential corresponds to a 100% loss of fluorescence.

### Online supplemental materials

Supplemental materials are available online at <http://www.jcb.org/cgi/content/full/jcb.200203043/DC1>. These materials include movies of IRM-correlated calcium elevations, the localization of EGFP-actin, ZAP-70-EGFP, LAT-EGFP, Grb2-EGFP, EYFP-Gads, and SLP-76-EYFP during TCR-induced spreading, as well as FRAP and inhibitor studies.

We thank Susan Garfield for her help in the operation of the LSM 510, Ms. V. Kapoor for help in the establishment of stable cell lines, Dr. J. Donaldson for providing the Tac-EGFP chimera, and Drs. J. Lippincott-Schwartz, P. Schwartzberg, and C. Sommers for reading the manuscript.

S.C. Bunnell is a Fellow of the Cancer Research Institute. D.I. Hong was a Howard Hughes Medical Institute-National Institutes of Health Research Scholar.

Submitted: 8 March 2002  
 Revised: 23 August 2002  
 Accepted: 27 August 2002

## References

- Allenspach, E.J., P. Cullinan, J. Tong, Q. Tang, A.G. Tesciuba, J.L. Cannon, S.M. Takahashi, R. Morgan, J.K. Burkhardt, and A.I. Sperling. 2001. ERM-dependent movement of CD43 defines a novel protein complex distal to the immunological synapse. *Immunity*. 15:739–750.
- Anton van der Merwe, P., S.J. Davis, A.S. Shaw, and M.L. Dustin. 2000. Cytoskeletal polarization and redistribution of cell-surface molecules during T cell antigen recognition. *Semin. Immunol.* 12:5–21.
- Balamuth, F., D. Leitenberg, J. Unternaehrer, I. Mellman, and K. Bottomly. 2001. Distinct patterns of membrane microdomain partitioning in Th1 and Th2 cells. *Immunity*. 15:729–738.
- Boniface, J.J., J.D. Rabinowitz, C. Wulfling, J. Hampl, Z. Reich, J.D. Altman, R.M. Kantor, C. Beeson, H.M. McConnell, and M.M. Davis. 1998. Initiation of signal transduction through the T cell receptor requires the multivalent engagement of peptide/MHC ligands. *Immunity*. 9:459–466.
- Brdicka, T., D. Pavlistova, A. Leo, E. Bruyns, V. Korinek, P. Angelisova, J. Scherer, A. Shevchenko, I. Hilgert, J. Cerny, et al. 2000. Phosphoprotein associated with glycosphingolipid-enriched microdomains (PAG), a novel ubiquitously expressed transmembrane adaptor protein, binds the protein tyrosine kinase csk and is involved in regulation of T cell activation. *J. Exp. Med.* 191:1591–1604.
- Bubeck Wardenburg, J., R. Pappu, J.Y. Bu, B. Mayer, J. Chernoff, D. Straus, and A.C. Chan. 1998. Regulation of PAK activation and the T cell cytoskeleton by the linker protein SLP-76. *Immunity*. 9:607–616.
- Bunnell, S.C., M. Diehn, M.B. Yaffe, P.R. Findell, L.C. Cantley, and L.J. Berg. 2000. Biochemical interactions integrating Itk with the T cell receptor-initiated signaling cascade. *J. Biol. Chem.* 275:2219–2230.
- Bunnell, S.C., V. Kapoor, R.P. Tribble, W. Zhang, and L.E. Samelson. 2001. Dynamic actin polymerization drives T cell receptor-induced spreading: a role for the signal transduction adaptor LAT. *Immunity*. 14:315–329.
- Daaka, Y., L.M. Luttrell, S. Ahn, G.J. Della Rocca, S.S. Ferguson, M.G. Caron, and R.J. Lefkowitz. 1998. Essential role for G protein-coupled receptor endocytosis in the activation of mitogen-activated protein kinase. *J. Biol. Chem.* 273:685–688.
- Delon, J., and R.N. Germain. 2000. Information transfer at the immunological synapse. *Curr. Biol.* 10:R923–R933.
- Delon, J., N. Bercovici, R. Liblau, and A. Trautmann. 1998. Imaging antigen recognition by naive CD4+ T cells: compulsory cytoskeletal alterations for the triggering of an intracellular calcium response. *Eur. J. Immunol.* 28:716–729.
- Delon, J., K. Kaibuchi, and R.N. Germain. 2001. Exclusion of CD43 from the immunological synapse is mediated by phosphorylation-regulated relocation of the cytoskeletal adaptor moesin. *Immunity*. 15:691–701.
- Dustin, M.L., and J.A. Cooper. 2000. The immunological synapse and the actin cytoskeleton: molecular hardware for T cell signaling. *Nat. Immunol.* 1:23–29.
- Finco, T.S., T. Kadlecik, W. Zhang, L.E. Samelson, and A. Weiss. 1998. LAT is required for TCR-mediated activation of PLC $\gamma$ 1 and the Ras pathway. *Immunity*. 9:617–626.
- Grakoui, A., S.K. Bromley, C. Sumen, M.M. Davis, A.S. Shaw, P.M. Allen, and M.L. Dustin. 1999. The immunological synapse: a molecular machine controlling T cell activation. *Science*. 285:221–227.
- Gruenberg, J., and F.R. Maxfield. 1995. Membrane transport in the endocytic pathway. *Curr. Opin. Cell Biol.* 7:552–563.
- Harder, T., and M. Kuhn. 2000. Selective accumulation of raft-associated membrane protein LAT in T cell receptor signaling assemblies. *J. Cell Biol.* 151:199–208.
- Holowka, D., E.D. Sheets, and B. Baird. 2000. Interactions between Fc( $\epsilon$ )RI and lipid raft components are regulated by the actin cytoskeleton. *J. Cell Sci.* 113:1009–1019.
- Hopkins, C.R., and I.S. Trowbridge. 1983. Internalization and processing of transferrin and the transferrin receptor in human carcinoma A431 cells. *J. Cell Biol.* 97:508–521.
- Janes, P.W., S.C. Ley, and A.I. Magee. 1999. Aggregation of lipid rafts accompanies signaling via the T cell antigen receptor. *J. Cell Biol.* 147:447–461.
- Johnson, K.G., S.K. Bromley, M.L. Dustin, and M.L. Thomas. 2000. A supramolecular basis for CD45 tyrosine phosphatase regulation in sustained T cell activation. *Proc. Natl. Acad. Sci. USA*. 97:10138–10143.
- Jung, K.Y., M. Takeda, D.K. Kim, A. Tojo, S. Narikawa, B.S. Yoo, M. Hosoyamada, S.H. Cha, T. Sekine, and H. Endou. 2001. Characterization of ochratoxin A transport by human organic anion transporters. *Life Sci.* 69:2123–2135.
- Kawabuchi, M., Y. Satomi, T. Takao, Y. Shimonishi, S. Nada, K. Nagai, A. Tarakhovskiy, and M. Okada. 2000. Transmembrane phosphoprotein Cbp regulates the activities of Src-family tyrosine kinases. *Nature*. 404:999–1003.
- Keller, P., D. Toomre, E. Diaz, J. White, and K. Simons. 2001. Multicolour imaging of post-Golgi sorting and trafficking in live cells. *Nat. Cell Biol.* 3:140–149.
- Koretzky, G.A., and P.S. Myung. 2001. Positive and negative regulation of T-cell activation by adaptor proteins. *Nat. Rev. Immunol.* 1:95–107.
- Krause, M., A.S. Sechi, M. Konrad, D. Monner, F.B. Gertler, and J. Wehland. 2000. Fyn-binding protein (Fyb)/SLP-76-associated protein (SLAP), Ena/vasodilator-stimulated phosphoprotein (VASP) proteins and the Arp2/3 complex link T cell receptor (TCR) signaling to the actin cytoskeleton. *J. Cell Biol.* 149:181–194.
- Krummel, M.F., and M.M. Davis. 2002. Dynamics of the immunological synapse: finding, establishing and solidifying a connection. *Curr. Opin. Immunol.* 14:66–74.
- Krummel, M.F., M.D. Sjaastad, C. Wulfling, and M.M. Davis. 2000. Differential clustering of CD4 and CD3 $\zeta$  during T cell recognition. *Science*. 289:1349–1352.
- Lee, K.H., A.D. Holdorf, M.L. Dustin, A.C. Chan, P.M. Allen, and A.S. Shaw. 2002. T cell receptor signaling precedes immunological synapse formation. *Science*. 295:1539–1542.
- Liu, K.Q., S.C. Bunnell, C.B. Gurniak, and L.J. Berg. 1998. T cell receptor-initiated calcium release is uncoupled from capacitative calcium entry in Itk-deficient T cells. *J. Exp. Med.* 187:1721–1727.
- Liu, S.K., N. Fang, G.A. Koretzky, and C.J. McGlade. 1999. The hematopoietic-specific adaptor protein gads functions in T-cell signaling via interactions with the SLP-76 and LAT adaptors. *Curr. Biol.* 9:67–75.
- Monks, C.R., B.A. Freiberg, H. Kupfer, N. Sciaky, and A. Kupfer. 1998. Three-dimensional segregation of supramolecular activation clusters in T cells. *Nature*. 395:82–86.
- Mu, F.T., J.M. Callaghan, O. Steele-Mortimer, H. Stenmark, R.G. Parton, P.L. Campbell, J. McCluskey, J.P. Yeo, E.P. Tock, and B.H. Toh. 1995. EEA1, an early endosome-associated protein. EEA1 is a conserved alpha-helical peripheral membrane protein flanked by cysteine “fingers” and contains a calmodulin-binding IQ motif. *J. Biol. Chem.* 270:13503–13511.
- Nakamura, N., M. Lowe, T.P. Levine, C. Rabouille, and G. Warren. 1997. The vesicle docking protein p115 binds GM130, a cis-Golgi matrix protein, in a mitotically regulated manner. *Cell*. 89:445–455.
- Negulescu, P.A., T.B. Krasieva, A. Khan, H.H. Kerschbaum, and M.D. Cahalan. 1996. Polarity of T cell shape, motility, and sensitivity to antigen. *Immunity*. 4:421–430.
- Prescott, A.R., J.M. Lucocq, J. James, J.M. Lister, and S. Ponnambalam. 1997. Distinct compartmentalization of TGN46 and beta 1,4-galactosyltransferase in HeLa cells. *Eur. J. Cell Biol.* 72:238–246.
- Richie, L.L., P.J. Ebert, L.C. Wu, M.F. Krummel, J.J. Owen, and M.M. Davis. 2002. Imaging synapse formation during thymocyte selection: inability of CD3 $\zeta$  to form a stable central accumulation during negative selection. *Immunity*. 16:595–606.
- Samelson, L.E. 2002. Signal transduction mediated by the T cell antigen receptor: the role of adaptor proteins. *Annu. Rev. Immunol.* 20:371–394.
- Shaw, A., and M.L. Dustin. 1997. Making the T cell receptor go the distance: a topological view of T cell activation. *Immunity*. 6:361–369.
- Sloan-Lancaster, J., J. Presley, J. Ellenberg, T. Yamazaki, J. Lippincott-Schwartz, and L.E. Samelson. 1998. ZAP-70 association with T cell receptor  $\zeta$  (TCR $\zeta$ ): fluorescence imaging of dynamic changes upon cellular stimulation. *J. Cell Biol.* 143:613–624.
- Sperling, A.I., J.R. Sedy, N. Manjunath, A. Kupfer, B. Ardman, and J.K. Burkhardt. 1998. TCR signaling induces selective exclusion of CD43 from the T cell-antigen-presenting cell contact site. *J. Immunol.* 161:6459–6462.
- Strous, G.J., and R. Govers. 1999. The ubiquitin-proteasome system and endocytosis. *J. Cell Sci.* 112:1417–1423.
- Ullrich, O., S. Reinsch, S. Urbe, M. Zerial, and R.G. Parton. 1996. Rab11 regulates recycling through the pericentriolar recycling endosome. *J. Cell Biol.* 135:913–924.
- Wilson, B.S., J.R. Pfeiffer, Z. Surviladze, E.A. Gaudet, and J.M. Oliver. 2001. High resolution mapping of mast cell membranes reveals primary and secondary domains of Fc $\epsilon$ RI and LAT. *J. Cell Biol.* 154:645–658.
- Wu, J., D.G. Motto, G.A. Koetzky, and A. Weiss. 1996. Vav and SLP-76 interact and functionally cooperate in IL-2 gene activation. *Immunity*. 4:593–602.
- Wulfling, C., and M.M. Davis. 1998. A receptor/cytoskeletal movement triggered by costimulation during T cell activation. *Science*. 282:2266–2269.

- Xavier, R., T. Brennan, Q. Li, C. McCormack, and B. Seed. 1998. Membrane compartmentation is required for efficient T cell activation. *Immunity*. 8:723–732.
- Yablonski, D., and A. Weiss. 2001. Mechanisms of signaling by the hematopoietic-specific adaptor proteins, SLP-76 and LAT and their B cell counterpart, BLNK/SLP-65. *Adv. Immunol.* 79:93–128.
- Yablonski, D., M.R. Kuhne, T. Kadlecsek, and A. Weiss. 1998. Uncoupling of non-receptor tyrosine kinases from PLC-gamma1 in an SLP-76- deficient T cell. *Science*. 281:413–416.
- Yablonski, D., T. Kadlecsek, and A. Weiss. 2001. Identification of a phospholipase C- $\gamma$ 1 (PLC- $\gamma$ 1) SH3 domain-binding site in SLP-76 required for T-cell receptor-mediated activation of PLC- $\gamma$ 1 and NFAT. *Mol. Cell. Biol.* 21:4208–4218.
- Yamazaki, T., K. Zaal, D. Hailey, J. Presley, J. Lippincott-Schwartz, and L.E. Samelson. 2002. Role of Grb2 in EGF-stimulated EGFR internalization. *J. Cell Sci.* 115:1791–1802.
- Zal, T., M.A. Zal, and N.R. Gascoigne. 2002. Inhibition of T cell receptor-coreceptor interactions by antagonist ligands visualized by live FRET imaging of the T-hybridoma immunological synapse. *Immunity*. 16:521–534.
- Zhang, W., B.J. Irvin, R.P. Tribble, R.T. Abraham, and L.E. Samelson. 1999. Functional analysis of LAT in TCR-mediated signaling pathways using a LAT-deficient Jurkat cell line. *Int. Immunol.* 11:943–950.
- Zhang, W., J. Sloan-Lancaster, J. Kitchen, R.P. Tribble, and L.E. Samelson. 1998a. LAT: the ZAP-70 tyrosine kinase substrate that links T cell receptor to cellular activation. *Cell*. 92:83–92.
- Zhang, W., R.P. Tribble, and L.E. Samelson. 1998b. LAT palmitoylation: its essential role in membrane microdomain targeting and tyrosine phosphorylation during T cell activation. *Immunity*. 9:239–246.